



Identification of Aquifer Layers Using Geoelectric Resistivity Method in Jono Oge Village, Sigi Biromaru District, Sigi District

M.D.T. Musa, Jamidun*, Sandra, and Dinda Anita Putri

Geophysical Engineering Study Program, Department of Physics, Faculty of Mathematics and Natural Sciences, Tadulako University

Information

Article history:

Received: 08 November 2023

Accepted: 02 June 2024

Published: 09 June 2024

Keywords:

*Geoelectric Barrier Types
Wenner Configuration
Aquifer Layers*

Abstract

Research has been carried out with the title "Identification of Aquifer Layers Using Geoelectrical Barrier Type Methods in Jono Oge Village, Sigi Biromaru District, Sigi Regency" aimed at finding out the distribution of aquifer layers in Jono Oge Village, Sigi Biromaru District, Sigi Regency after liquefaction caused by the earthquake on 28 September 2018. This research uses Automatic Array Scanning (AAS) method with Wenner configuration with a total of 5 passes. Data processing uses the Res2dinv software program. Data collection was carried out on 5 tracks, with a total length of each measurement track of 240 meters. The results obtained show that the aquifer layer has a specific resistance value of 59.70 - 149.24 Ωm with a formation factor value of 2 - 5, it is thought to be an aquifer layer consisting of sand and gravel shown in green. This layer is at a depth of $\pm 18 - 39$ m below the ground surface with a thickness of around $\pm 10 - 20$ m, so this aquifer layer is thought to have experienced a decrease or change in depth of around ± 10 m Bmt after the liquefaction disaster.

*) e-mail: midungeofisik@gmail.com

DOI: 10.22487/gravitasi.v22i2.16679

1. INTRODUCTION

The Palu earthquake on September 28 2018 had a magnitude of Mw 7.4 which was caused by the activity of the Palu Koro Fault [1]. This fault passes through the Palu Valley and Koro Valley to the northern part of Bone Bay for 250 km [2]. The earthquake damaged residents' houses and infrastructure, caused many human casualties and triggered other disasters such as liquefaction. Liquefaction is a phenomenon of loss of soil strength due to vibration earthquake.

When experiencing vibration, pore water exerts pressure on the soil particles, thereby affecting the density of the soil [3]. The liquefaction phenomenon can occur if it meets the requirements, such as the sediment layer being sand (non-cohesive), being decomposed or loose (not solid), being below the ground water level or saturated with water, and a strong and long-lasting earthquake occurs [4]. One of the areas affected by liquefaction due to this earthquake is Jono Oge Village, Sigi Biromaru District, Sigi Regency. Based on observations and interpretation results carried out by LAPAN, it was noted that ± 209.9 Ha in Jono Oge Village was affected by liquefaction. The number of buildings affected was 689 of which 412 buildings were damaged and 277 other buildings were categorized as possibly damaged buildings [5]. Apart from that, the Gumbasa Irrigation water channel was damaged and is currently still in the process of being repaired. Based on information obtained from the Head of Jono Oge Village, the groundwater level in Jono Oge Village before liquefaction was at a depth of ± 2 meters. Thus, this area has the potential for

liquefaction. Liquefaction disasters may also change subsurface layers such as the position of the groundwater layer, so research needs to be carried out to see changes in the position of the groundwater layer (aquifer). Based on information from the community, local residents obtain water at a depth of ± 15 m. An aquifer is a subsurface layer that can store and transmit water [6]. Aquifers are available in quite large quantities and are of excellent quality. One geophysical method that can determine the aquifer layer is the type resistance geoelectric method. The geoelectric method is a geophysical method that can be used to determine aquifer layers. The type resistance geophysical method is an exploration method that utilizes the type resistance properties of materials located below the earth's surface. The measurement results will reveal the resistivity value at that depth. This method has previously been used by Ni Komang Puspitasari [7], Murniasih [8], and Dian Wahyuni [9] to determine the groundwater layer (aquifer) based on its type resistance value. The aim of this research is to determine the existence and depth of the aquifer layer in Jono Oge Village, Sigi Biromaru District, Sigi Regency after liquefaction due to the 28 September 2018 earthquake.

Based on the Geological Map Review of Palu Sheet Scale 1:250,000 [10], the rock stratigraphy of the research location and its surroundings is composed of 3 rock formations, namely the Alluvium Formation and Beach Deposits (Qap). This formation consists of sandstone, gravel, mud and coral limestone. Apart from that, in the eastern part of the research



location there are the Molasa Celebes Sarasin and Sarasin Formations. This formation consists of conglomerate, sandstone, mudstone, coral limestone and marl, and there is a Metamorphic Rock Complex Formation (Km), which can be seen in Figure 1.

$$F = \rho / \rho_w \tag{2}$$

Table 1 below is a summary of the rock formation factor (F) values from several hydrogeological studies that have been carried out.

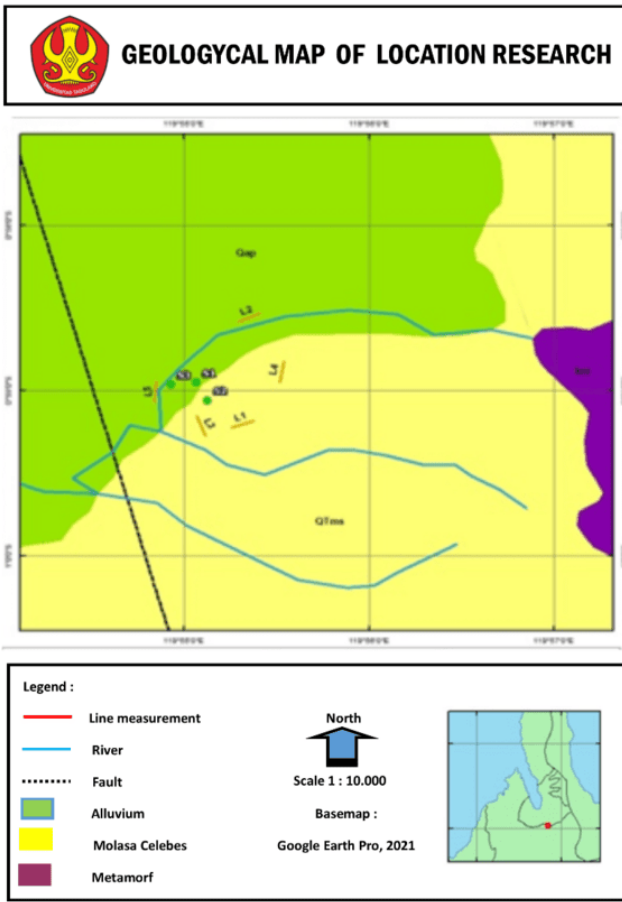


Figure 1 Geological map of the research location and its surroundings

. Groundwater is water that moves in the soil in the spaces between soil grains which seeps into the soil and moves to form a layer of soil called an aquifer [11]. Based on the distribution of aquifers and non-aquifers below the ground surface, it is recognized that there are aquifer systems as follows, namely unconfined aquifers, which are water-free layers that are only partially filled with water and are above the impermeable layer, confined aquifers, which are confined aquifers. the entire amount of water is limited by the waterproof layer, both above and below. Semi-confined aquifer is an aquifer in which the water pressure is completely saturated. Semi unconfined aquifer is an aquifer whose bottom is a waterproof layer, while the top is a fine-grained material so that the covering layer still allows water movement [12]. In hydrogeological exploration, resistance measurements can be calculated using Equation (1):

$$\rho_w = 10000 / EC. \tag{1}$$

where EC = electrical conductivity.

Based on Equation (1), the value of the formation factor (F) can be calculated using Equation (2) below:

Table 1 Classification of formation factor estimates for sedimentary rocks [13].

F	Formation	Aquifer/Aquiclude
≤ 1	Aquiclude Clay	Aquiclude Clay
1-1,5	Peat, clay sand, or Aquiclude silt	Aquiclude silt
2	Silt – fine sand Slight	moderate aquifer
3	Medium sand Medium	productive aquifer
4	Coarse sand	Productive aquifer
5	Gravel	Aquifers are very productive

The geoelectric method is a method that uses the principle of electric current flow to investigate subsurface rock structures. Geoelectric methods can be used in hydrogeological investigations such as determining aquifers and the presence of contamination, mineral investigations, archaeological surveys and hotrocks detection in geothermal investigations [14].

Geoelectric resistance is one of the methods commonly used to determine the resistance value of a rock layer below the surface [15]. This method uses direct current (DC) electricity with high voltage into the ground. Through the current electrode namely C1 and C2 which are plugged into the ground at a certain distance, an electric current is injected. The electric potential produced by the two current sources is the potential difference measured at 2 potential measurement points, namely P1 and P2, as in Figure 2.

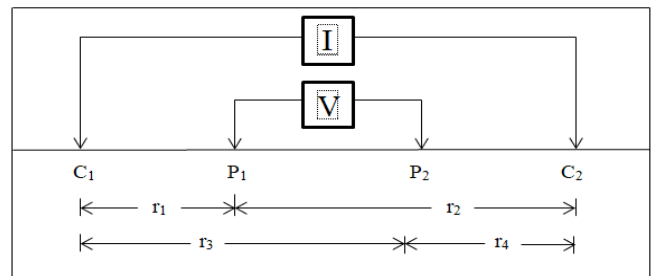


Figure 2 Arrangement of current and potential electrodes in geoelectric method measurements [16]

From the magnitude of the measured current and potential difference, the type resistance value can be calculated using the equation:

$$\rho_a = \frac{2\pi}{\left\{ \left(\frac{1}{r_1} - \frac{1}{r_2} \right) \left(\frac{1}{r_3} - \frac{1}{r_4} \right) \right\}} \frac{\Delta V}{I} \tag{3}$$

The measured type resistance is actually the apparent type resistance (ρ_a). The magnitude of the apparent resistance (ρ_a) is:

$$\rho_a = K \frac{V}{I} \tag{4}$$

ρ_a = Calculation result of resistivity value; V = potential difference, and I values of measured current strength

The Automatic Array Scanning (AAS) method is a geoelectric resistance-type method that carries out repeated and sequential measurements using a certain penetration depth. This method is often also referred to as Electrical Resistivity Tomography (ERT). The definition of ERT is a multi-electrode geoelectric method used to obtain information about the condition of materials below the ground surface based on the distribution pattern of the values resistivity of materials below the ground surface [17].

The Wenner configuration is one of the configurations in the geoelectric method, where the electrodes have the same spacing ($r_1=r_4=a$ and $r_2=r_3=2a$). The current electrode has a distance of 3 times the distance of the potential electrode, while the distance between the potential electrode and the sounding point is $a/2$, so the distance between the current electrode and the sounding point is $3a/2$. So that the depth that can be achieved is $a/2$.

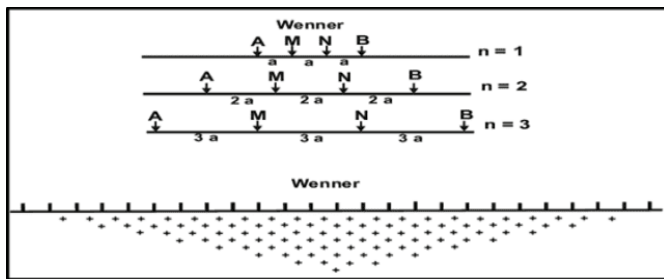


Figure 3 Wenner configuration electrode arrangement

Based on the electrode arrangement in the Wenner configuration, the following geometric factors are obtained:

$$K = 2\pi \{ (1/r_1 - 1/r_2) - (1/r_3 - 1/r_4) \} \tag{5}$$

or

$$K = 2\pi a \tag{6}$$

2. RESEARCH METHOD

This research area is in Jono Oge Village, Sigi Biromaru District, Sigi Regency. Geographically, the research location is located at 119°54'14.4" - 119°55'44.4" East Longitude and 00°58'15" - 00°59'30" South Latitude. The measurement point area can be seen in Figure 4.

The equipment used in this research is a set of geoelectric resistance measuring instruments, consisting of 4 cable rolls, main unit, 2 electric current sources (batteries), connecting cables, 25 electrodes, and electrode clamps. Global Positioning System (GPS) 1 piece, functions to determine the coordinates of the position of measuring points and height. 2 meters (100 m and 50 m), function to measure the length of the electrode spacing and the length of the path. 2 hammers, function to drive current electrodes and potential electrodes into the ground. Stationery and data tables function to input measurement data. The laptop functions to process data obtained from measurements in the field. Conductivitymeter, to measure the Electrical Conductivity (EC) of water. Arcgis 10.8, to create maps. Palu Sheet Geological Map, Scale 1 : 250,000, to create a geological map of the research area and supporting data for the data interpretation process. Google Earth map, as a basic map of the measurement trajectory.

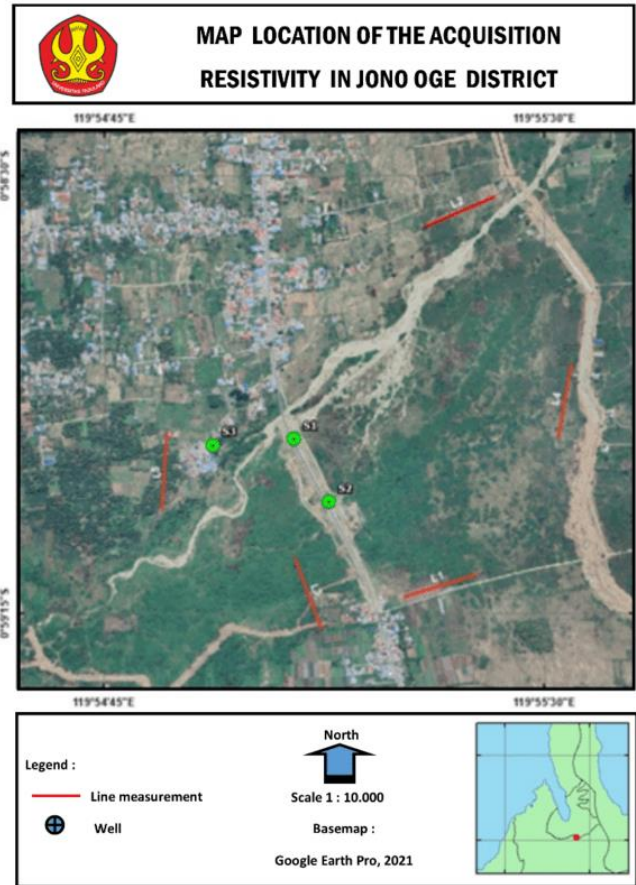


Figure 4 Map of research location

The measurement procedure in the field is to carry out a preliminary survey to obtain an overview of the geological and topographic conditions of the research area and determine the location of geoelectric measurement locations. The next step is to assemble the georesistivity meter and main unit, by connecting 25 cables and electrodes with a spacing of 10 m. After assembling the device, then inject current into the ground to get the current (I) and potential difference (V), then take the coordinates of each electrode. Measurements were carried out using the Automatic Array Scanning (AAS) method with a Wenner configuration. The number of trajectories is 5 trajectories, consisting of 25 electrodes. The spacing between electrodes is 10 m, so the path length reaches 240 m. This measurement was carried out to obtain an overview of the topography of each track.

Table 2 Results of EC measurements and calculation of pore-filling water type resistance

Well	Well coordinate	EC ($\mu\text{S/cm}$)	ρ_w (Ωm)	Explanation
1	0°58'57.04" 119°55'07.67"	280	35.71	Dug-well belong to PT. WIKA with the depth of 12 m, cloudy, bad smell
2	0°59'03.51" 119°55'07.67"	272	36.76	Dug-well belong to PT. WIKA with the depth of 12 m, cloudy, bad smell
3	0°58'57.73" 119°54'55.81"	586	17.06	Boring-well belong to the resident with the depth of 15 m, clear, no smell

Next, to support the interpretation stage, water samples were taken from 2 dug wells owned by WIKA (Wijaya Karya) and 1 drilled well owned by residents, then measured the Electrical Conductivity (EC) of the water which was used to calculate the resistance value of the type of pore-filling water (ρ_w) using Equation (1). Then, the pore-filling water type resistance value (ρ_w) is used to calculate the value rock formation factors using Equation (2).

3. RESULTS AND DISCUSSION

Results and Data Processing

The results of water EC measurements and calculations of pore-filling water type resistance can be seen in Table 2. The software used to process the data is Res2dinv by entering the

apparent type resistance value (ρ_a), electrode spacing, datum value and electrode elevation. The result of this processing is a 2D cross-section of subsurface type obstacles, which consists of 3 resistivity cross-sections. The first section shows the measured apparent resistivity, the second section shows the calculated apparent resistivity and the third section shows the actual resistance section obtained through the inversion modeling process (inverted resistivity section). Information on the third cross section is in the form of color differences which indicate the type resistance value. In data processing, iterated 5 times to reduce the root mean squared error (RMS) value.

The following displays the results of 2D modeling of subsurface obstacles.

1. Path 1

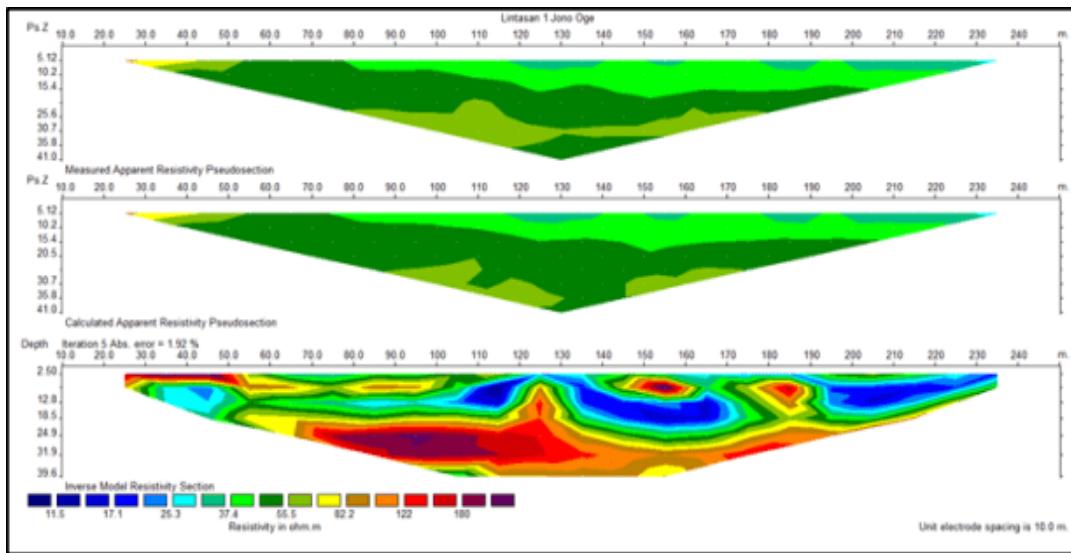


Figure 5 2D Cross-section of Path 1

2. Path 2

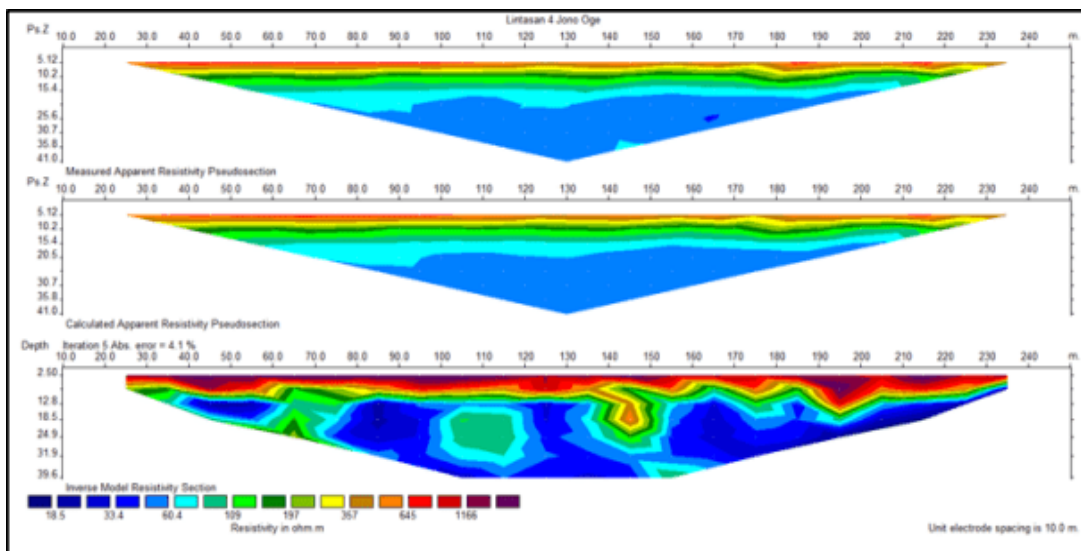


Figure 6 2D Cross-section of Path 2

Based on Figure 5, the third cross section (inverse resistivity section) shows the value of the lowest to highest type resistance range of $10.44 \Omega\text{m} - 294.83 \Omega\text{m}$. The depth obtained reached 39.6 m bgl (below ground level), with an error rate of 1.9% through 5 iteration processes. Based on Figure 6, the

third cross section (inverse resistivity section) shows the value of the lowest to highest type resistance range of $15.94 \Omega\text{m} - 2443.20 \Omega\text{m}$. The depth obtained reached 39.6 m bgl (below ground level), with an error rate of 4.1% through 5 iteration processes.

3. Path 3

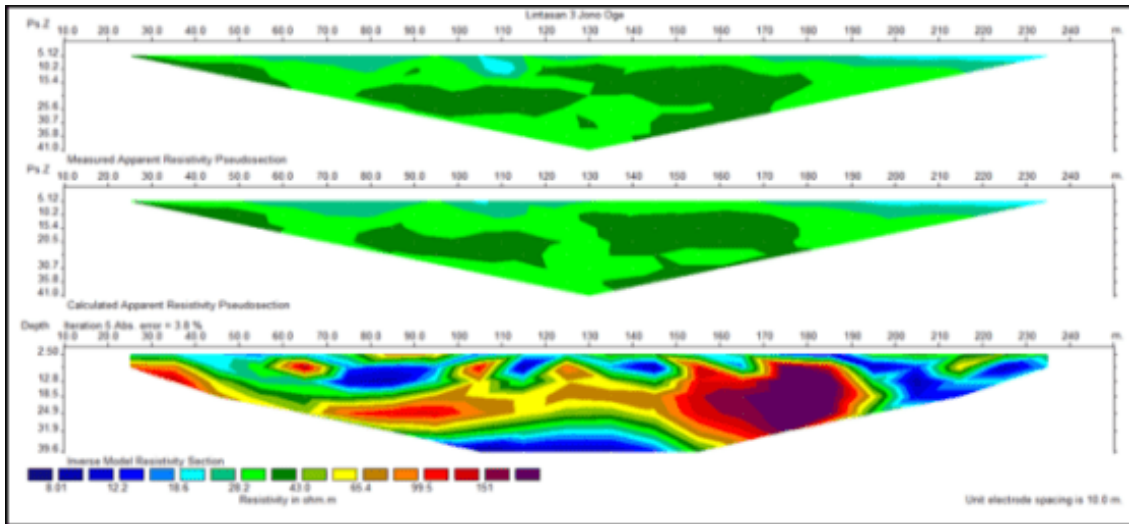


Figure 7 2D Cross-section of Path 3

4. Path 4

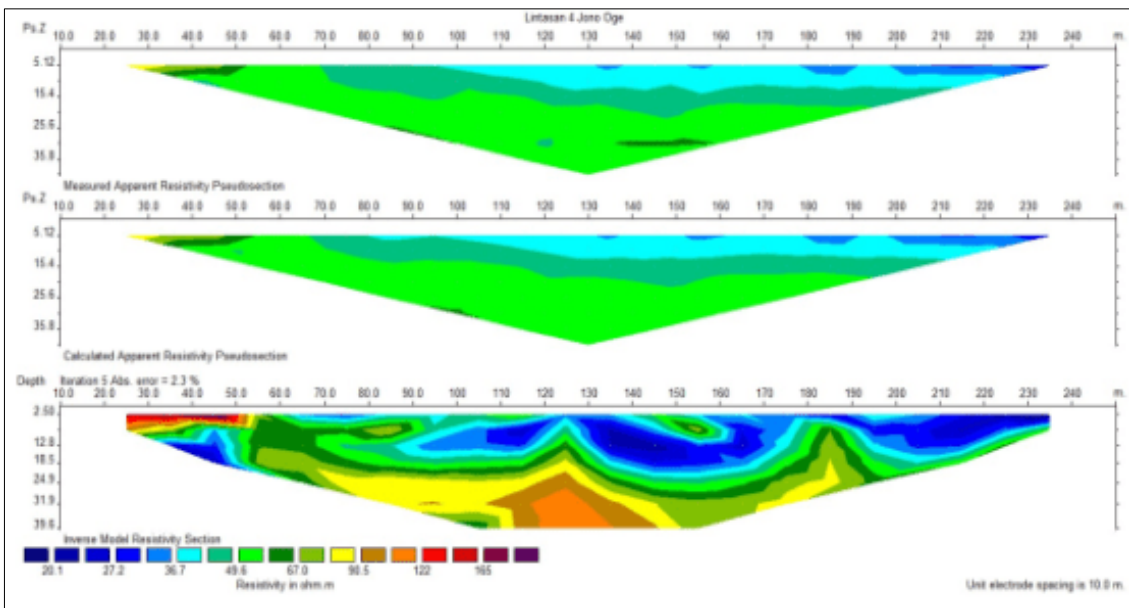


Figure 8 2D Cross-section of Path 4

Based on Figure 7, the third cross section (inverse resistivity section) shows the value of the lowest to highest type resistance range of $7.25 \Omega\text{m} - 255.96 \Omega\text{m}$. The depth obtained reached 39.6 m bmt, with an error rate of 3.8% through 5 iteration processes. Based on Figure 8, the third cross section (inverse resistivity section) shows the value of the lowest to highest type resistance range of $18.66 \Omega\text{m} - 240.68 \Omega\text{m}$. The depth obtained reached 39.6 m bgl (below ground level), with an error rate of 2.3% through 5 iteration processes. Based on Figure 9, the third cross section (inverse resistivity section) shows the value of the lowest to highest type resistance range of $5.28 \Omega\text{m} - 295.38 \Omega\text{m}$. The depth obtained reached 39.6 m bgl (below ground level), with an error rate of 4.5% through 5 iteration processes.

Interpreting the resistance value of the type of data processing results for each path requires other supporting data.

These data include the geological conditions of the research location, and EC measurement data. The measurement tracks at the research location are in 2 formations, namely the Alluvium and Beach Sediment Formations and the Molasa Celebes Sarasin and Sarasin Formations. Therefore, when estimating formation factors, the classification for sedimentary rocks is used (Table 1). Furthermore, from the results of EC data processing, the average value of the pore-filling water type resistance (ρ_w) was obtained, namely $29.85 \Omega\text{m}$ (Table 2) which was used to determine the formation factor value for each layer. By comparing these geological conditions with the formation factor values, a correlation is obtained between the type resistance values and the lithology of the research location.

5. Path 5

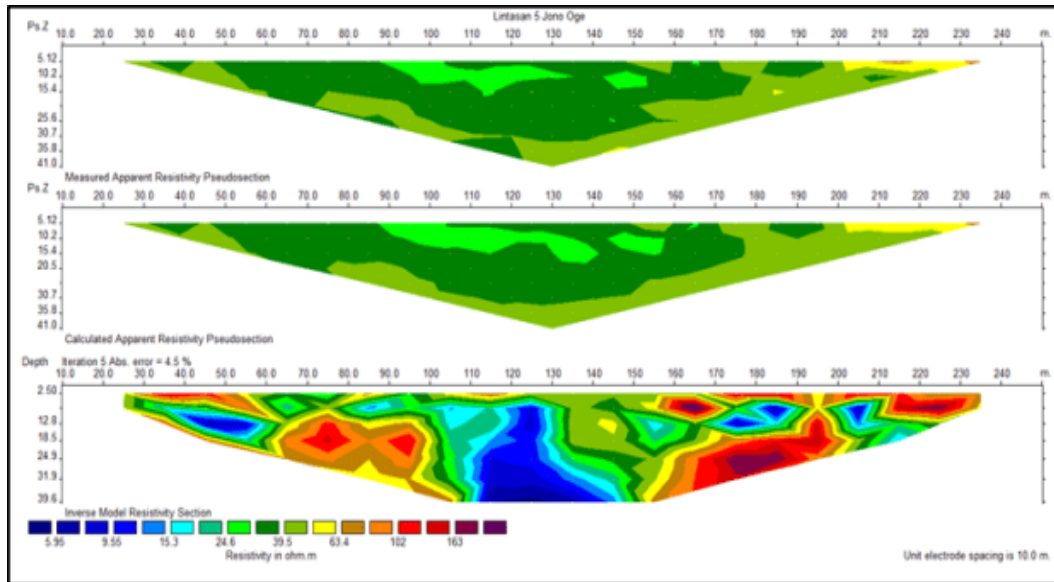


Figure 9 2D Cross-section of Path 5

In general, the type resistance values and formation factors obtained reflect the differences in subsurface layers which are interpreted as follows:

1. Layer 1 with a specific resistance value $< 59.70 \Omega\text{m}$ (yellow) with a formation factor < 2 , this layer is thought to be an aquitard layer consisting of soft clay and sandy clay with low permeability.
2. Layer 2 with a specific resistance value of $59.70 - 149.24 \Omega\text{m}$ (green) with a formation factor of $2 - 5$, this layer is thought to be is an aquifer layer consisting of fine sand,

medium sand, coarse sand and gravel. This layer is thought to be an aquifer layer.

3. Layer 3 with a specific resistance value $> 149.24 \Omega\text{m}$ (red) with a formation factor > 5 , this layer is thought to be an aquiclude layer consisting of sandstone with a low porosity value. This layer is impermeable (waterproof).

To obtain an overview of the subsurface aquifer layer, the entire cross-section of type barriers is interpreted through the following formation factor cross-section:

1. Path 1

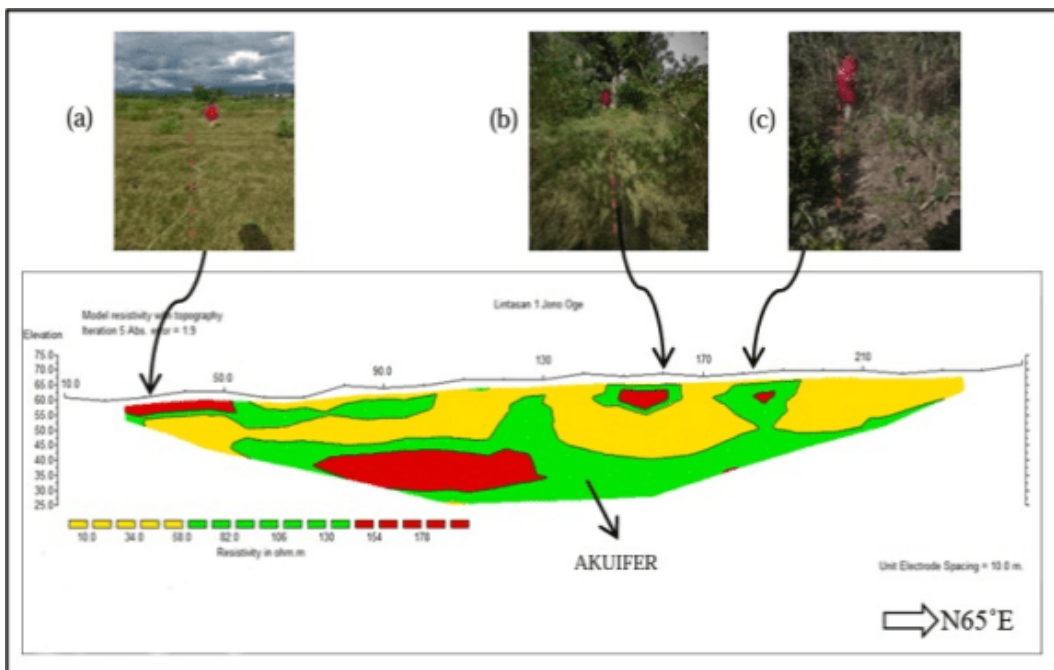


Figure 10 2D Cross-section of type obstacles with topographic correction on Path 1

Based on the cross-section of path 1 (Figure 10), it can be seen that there is Layer 2 which is thought to be a resistant aquifer layer of type $59.70 - 149.24 \Omega\text{m}$ with a formation factor of 2

$- 5$ (green). This layer was detected at a depth of $\pm 18 \text{ m}$ bgl (below ground level) with a thickness of $\pm 20 \text{ m}$ in clean conditions. At this location there is data on a dug well with a

depth of ± 12 m but it is cloudy and smells bad. The aquifer layer in this path thickens towards the southwest. At the top of the layer, Layer 3 was detected which was inserted from electrodes 3 – 5 with a thickness of ± 5 m and at electrodes 6 – 10, Layer 1 was detected along the track as seen in the insert of Figure 10, part a. Layers that have the same color and resistance value as the aquifer layer are visible at electrodes 3 – 5 and electrodes 15 – 16. These layers are in a shallower position than the aquifer layer and are shaped like small lenses which are also interspersed with Layer 3 with a thickness of ± 5 m as seen in the insert of Figure 10 parts b and c. It is suspected that this layer is Layer 1 which is in the form of clay

and sandy loam which has been affected by water infiltration from the surface.

Based on the cross-section of path 2 (Figure 11), it can be seen that there is Layer 2 which is thought to be an aquifer layer with resistance type 59.70 – 149.24 Ω m with a formation factor of 2 – 5 (green). This layer was detected at a depth of ± 18 m bgl (below ground level) with a thickness of ± 15 m. The aquifer layer on this track thickens towards the southwest. This layer is interspersed with Layer 1, where the surface of this layer is covered by Layer 3 (red layer) with a surface appearance as seen in the insert of Figure 11 parts a and b.

2. Path 2



Figure 11 2D Cross-section of type obstacles with topographic correction on Path 2

3. Path 3

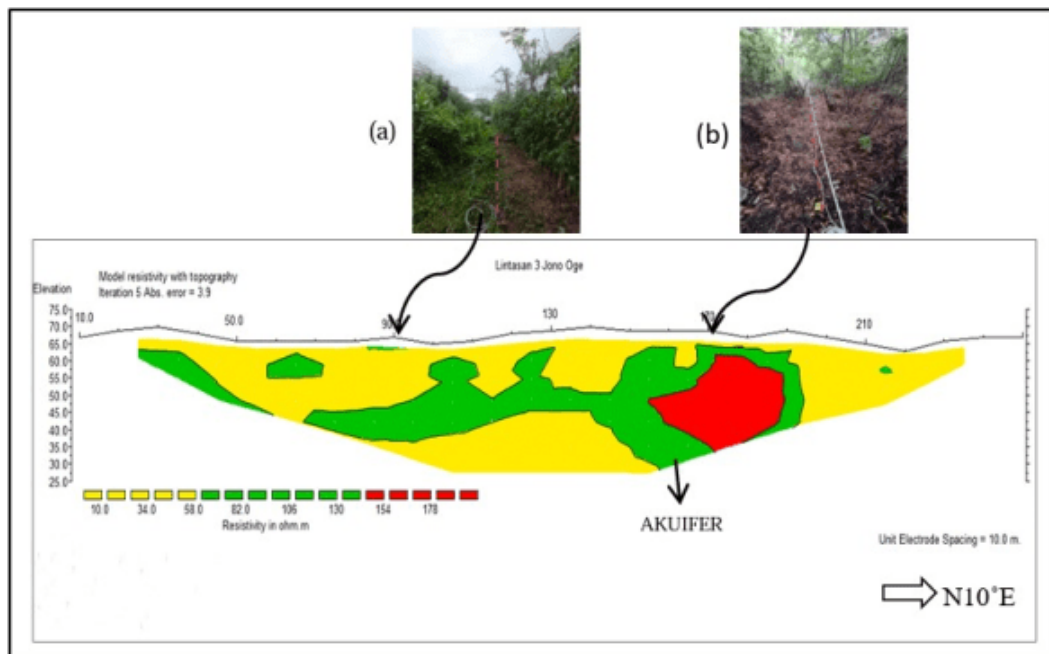


Figure 12 2D Cross-section of type obstacles with topographic correction on Path 3

Based on the cross-section of path 3 (Figure 12), it can be seen that there is Layer 2 which is thought to be a resistant aquifer layer of type 59.70 – 149.24 Ωm with a formation factor of 2 – 5 (green). This layer was detected at a depth of ± 18 m bgl (below ground level) with a thickness of ± 20 m. The aquifer layer on this track thickens towards the south. At the bottom of the layer, it was detected that Layer 3 was inserted from electrodes 15 – 19 with a thickness of ± 10 m and at the top, it was limited by Layer 1 along the track as seen in the insert image 12 part b. A layer that has the same color and resistance value as the aquifer layer is visible on the surface like small lenses on electrode 9, visible in the insert of Figure 12, part b. It is suspected that this layer is Layer 1 which is in the form of clay and sandy loam which has been affected by water infiltration from the surface.

Based on the cross-section of path 4 (Figure 13), it can be seen that there is Layer 2 which is thought to be a resistant aquifer layer of type 59.70 – 149.24 Ωm with a formation factor of 2 – 5 (green). This layer was detected at a depth of ± 18 m bgl (below ground level) with a thickness of ± 20 m. The aquifer layer on this track thickens towards the south. At the bottom of the layer, it was detected that Layer 3 was inserted from electrodes 8 – 13 with a thickness of ± 10 m and at the top, it was limited by Layer 1 along the track as seen in the insert of Figure 13, part b. Layers that have the same color and specific resistance value as the aquifer layer are visible on the surface like small lenses and are interspersed with Layer 3 of 3 – 5 and electrodes 15 – 16, as seen in the insert of Figure 13 parts a and c.

4. Path 4

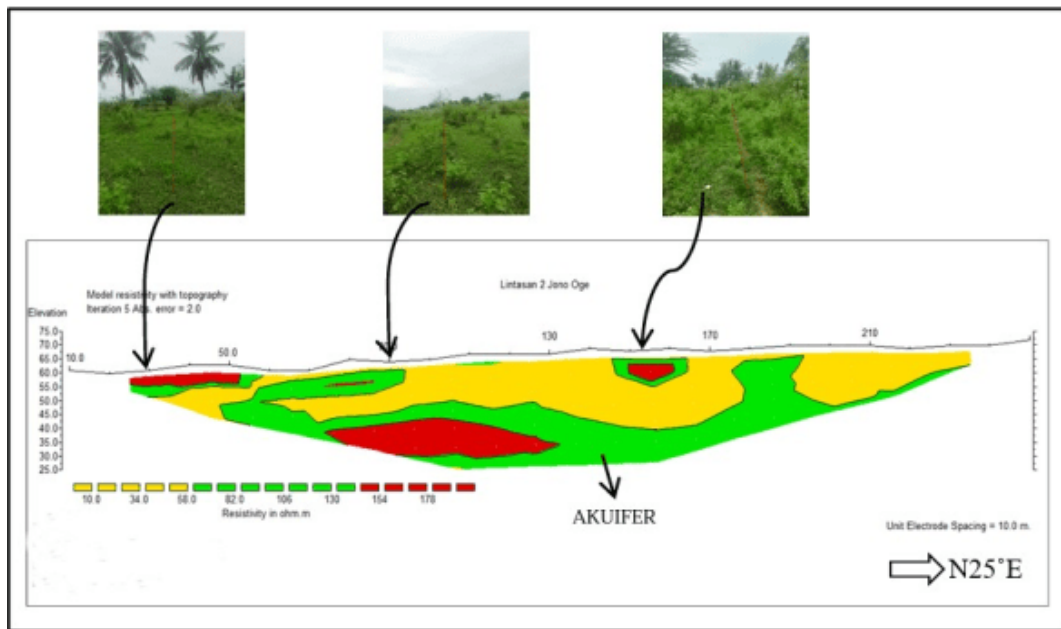


Figure 13 2D Cross-section of type obstacles with topographic correction on Path 4

5. Path 5

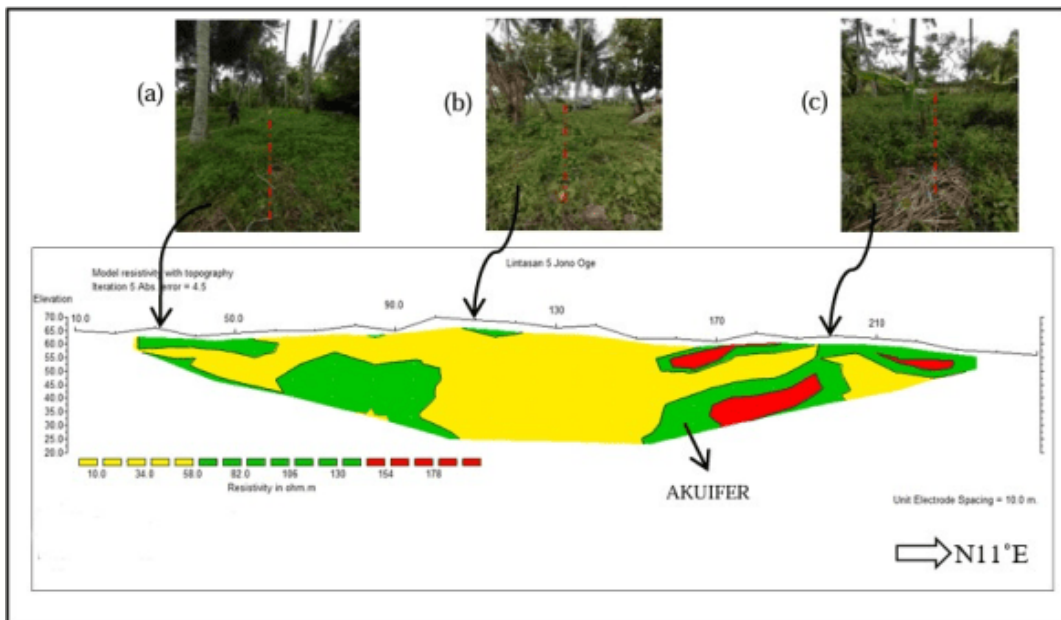


Figure 14 2D Cross-section of type obstacles with topographic correction on Path 5

Based on the cross-section of path 5 (Figure 14), it can be seen that there is Layer 2 which is thought to be an aquifer layer with resistance type 59.70 – 149.24 Ω m with a formation factor of 2 – 5 (green). This layer was detected at a depth of \pm 18 m bgl (below ground level) with a thickness of \pm 20 m. The aquifer layer on this track thickens towards the south. A layer that has the same color and type resistance value as the aquifer layer appears on the surface at electrodes 3 – 6, electrodes 11 – 12, and electrodes 17 – 23 with a depth of 5 – 10 m bgl (below ground level). This layer is in the shallowest position of the aquifer layer and is shaped like small lenses, and in the insert of Figure 14 part c is interspersed with Layer 3 with a thickness of \pm 5 m. It is suspected that this layer is Layer 1 which has been exposed to infiltration water around the measurement track and the surface condition of Layer 1 is not solid and dry, as seen in the insert of Figure 14 parts a, b and c.

4. CONCLUSION

Based on the research results, it can be concluded that the aquifer layer in Jono Oge Village, Sigi Biromaru District, Sigi Regency has a type resistance value ranging from 59.70 – 149.24 Ω m. It is thought that this layer consists of fine sand, medium sand, coarse sand and gravel that has a formation factor value of 2-5 which is a medium aquifer – productive aquifer is shown in green. This layer is at a depth that varies between \pm 18 to \pm 39 m. The aquifer layer thickens towards the south with a thickness ranging from \pm 10 to \pm 20 m. According to local residents, before experiencing liquefaction, the depth of groundwater in Jono Oge Village was at a depth of 4 – 6 m bgl (below ground level) This aquifer layer is thought to have decreased or changed the drilled wells and dug wells that people use for clean water, these wells are at a depth of around \pm 15 m bgl (below ground level) after the liquefaction disaster.

REFERENCES

- [1] [BMKG] Badan Meteorologi, Klimatologi, dan Geofisika (2018). *Monitoring Gempa Bumi 28 September 2018*. Diperoleh dari website. Badan Meteorologi, Klimatologi, dan Geofisika.
- [2] Abdullah. (1998). Penerapan Metode Gradien Gaya Berat dan Analisis Model 2-D Struktur Sesar Palu-Koro dan Sesar Janedo Kab. Donggala-Sulawesi Tengah. *Tesis*. Program Studi Geofisika Terapan. Institut Teknologi Bandung.
- [3] Mina, E., Kusuma, R. I., dan Sudirman, S. (2018). Analisa Potensi Likuifaksi Berdasarkan Data SPT (Studi Kasus proyek Pembangunan Gedung Baru Untirta Sindang Sari). *Jurnal Fondasi*, 7(1), 11-21.
- [4] Iqbal, P., Tohari, A., Sadisun, I.A., dan Nugroho, D. Fasies sedimen Kuartar berpotensi likuifaksi Pesisir Kota Padang, Provinsi Sumatera Barat berdasarkan data inti bor dan CPTu. *Jurnal Lingkungan dan Bencana Geologi*, 5(1), 1-18.
- [5] Pemerintah Sulawesi Tengah. (2018). *Master Plan for the Recovery and Rebuilding of the Post-Disaster Area of Central Sulawesi Province (Rencana Induk Pemulihan dan Pembangunan Kembali Wilayah Pascabencana Provinsi Sulawesi Tengah)*.
- [6] Hanifa, D., Sota, I., & Siregar, S. S. (2016). Penentuan Lapisan Akuifer Air Tanah Dengan Metode Geolistrik Konfigurasi Schlumberger Di Desa Sungai Jati Kecamatan Mataraman Kabupaten Banjar Kalimantan Selatan. *Jurnal Fisika FLUX*, 13(1), 30–39.
- [7] Puspitasari, N. K. (2020). Identifikasi Lapisan Akuifer Menggunakan Metode Geolistrik Hambatan Jenis Di Desa Pombewe Kabupaten Sigi. *Skripsi*. Prodi Fisika. Jurusan Fisika. Fakultas Matematika dan Ilmu Pengetahuan Alam, Universitas Tadulako. Palu.
- [8] Siti Murniasih. (2020). Identifikasi Lapisan Akuifer di Kelurahan Petobo Kota Palu Menggunakan Metode Geolistrik Hambatan Jenis. *Skripsi*. Prodi Fisika. Jurusan Fisika. Fakultas Matematika dan Ilmu Pengetahuan Alam. Universitas Tadulako. Palu.
- [9] Wahyuni, D., Musa, M. D. T., & Sandra, S. (2018). Identifikasi Sebaran Lapisan Akuifer Menggunakan Metode Geolistrik Hambatan Jenis di Wilayah Kecamatan Ampibabo Kabupaten Parigi Moutong. *Natural Science: Journal of Science and Technology*, 7(2), 176-186.
- [10] Soekamto, Rab. (1973). *Peta Geologi Tinjau Lembar Palu*. Bandung: Pusat Penelitian dan Pengembangan Geologi.
- [11] Unib, M. (2006). Sebaran Aquifer dan Pola Aliran Air Tanah di Kecamatan Batuceemper dan Kecamatan Benda Kota Tanggerang, Propinsi Banten. *Jurnal Geologi Indonesia*, 1(3), 115-128.
- [12] Kementerian Pekerjaan Umum dan Perumahan Rakyat. (2017). *Modul Geologi dan Hidrogeologi (Pelatihan Perencanaan Air Tanah)*. Bandung: Pusat Pendidikan dan Pelatihan Sumber Daya Air dan Konstruksi.
- [13] Taib, M.I.T. (1999). *Diktat Kuliah Eksplorasi Geolistrik, Departemen Teknik Geofisika*. Institut Teknologi Bandung. Bandung.
- [14] Rohim, M.N., Subagio, H., dan Hidayah, N. *Applikasi Metode Geolistrik Sounding Dengan Konfigurasi Pole-Pole Untuk Mengukur Resistivitas Bawah Permukaan Tanah Dan Mengetahui Struktur Tanah. PKM-GT, 10*. Universitas Negeri Malang.
- [15] Djuhaepa, A. P. (2015). Identifikasi Sebaran Bijih Besi dengan Menggunakan Metode Geolistrik Hambatan Jenis di Desa Ogowele Kabupaten Tolitoli. *Skripsi*. Prodi Fisika. Jurusan Fisika. Fakultas Matematika dan Ilmu Pengetahuan Alam. Universitas Tadulako. Palu.
- [16] Telford, W.M., Geldart, L.P. dan Sheiff, R.E. 1990. *Applied Geophysics 2nd Edition*. Cambridge: Cambridge University.
- [17] Lowrie, & William. (2007). *Fundamental of Geophysics (2nd ed.)*. NewYork: Cambridge University Press.